Power Transformer Condition Monitoring Based on Evaluating Oil Properties

Ivan V. Bryakin [1], **Igor V. Bochkarev** [2], **Vadim R. Khramshin** [3,*], **Vadim R. Gasiyarov** [4] and **Ivan V. Liubimov** [5]

1   Institute of Mechanical Engineering and Automation, National Academy of Sciences of the Kyrgyz Republic, Bishkek 720010, Kyrgyzstan; bivas2006@yandex.ru
2   Department of Electromechanics, Kyrgyz State Technical University named after I. Razzakov, Bishkek 720010, Kyrgyzstan; elmech@mail.ru
3   Power Engineering and Automated Systems Institute, Nosov Magnitogorsk State Technical University, 455000 Magnitogorsk, Russia
4   Department of Automation and Control, Moscow Polytechnic University, 107023 Moscow, Russia; gasiyarovvr@gmail.com
5   Department of Mechatronics and Automation, South Ural State University, 454080 Chelyabinsk, Russia; liubimoviv@susu.ru
*   Correspondence: hvrmgn@gmail.com; Tel.: +7-3519-22-17-19

Abstract: The authors review the techniques applied to diagnose oil aging. Further, the authors put forward a new diagnostic method. It stipulates for an additional high-frequency measuring loop formed in an operating transformer. This dielcometric measuring capacitor cell includes a stray capacitance generated by the transformer winding and core. The monitoring of the dependence between the physico–technological oil parameters and the measuring cell capacity is fundamental for the procedures for determining the composition and properties of the transformer oil filling this cell. High-frequency low-voltage is the output signal. To prevent the cross-impact of low-frequency high-voltage and high-frequency low-voltage circuits, the pilot high-frequency low-voltage is excited by a special coupling capacitor; the output to the power feeder is conducted through an appropriate low-frequency choke, where the measuring capacitor cell does not disturb the normal transformer operation. The key physical processes used for the monitoring are analyzed and described in detail. The authors develop an algorithm to compute the current resistances of both the transformer oil and its impurities. The transformer state is estimated by comparing the parameters specified with preset permissible limits. A structure flowchart based on two synchronous quadrature detectors is proposed for a high-frequency measuring loop. The monitoring system considered allows for determining the following insulating oil properties by using the algorithm for processing the recorded data: moisture content; dielectric losses due to the accumulation of aging products in the oil and its pollution; and the content of dissolved gases in the oil. The monitoring system operability and efficiency are confirmed by appropriate experimental studies. The experiments are conducted using a TM-25-6/0.4 oil-filled transformer with a capacity of 25 kVA in a steady-state operating mode at a load current of 25 A. It is found that the proposed control system allows for identifying a critical defect of increased moisture content in the oil with no more than 10% error, and a sensitivity threshold in the order of tenths of ppm.

Keywords: transformer; transformer oil; oil aging; pilot high-frequency low-voltage; coupling capacitor; measuring capacitor cell; complex winding resistance; complex permittivity; transformer oil resistance

1. Introduction

Today, power supply systems use many power transformers, which are the key energy system components designed to increase or decrease voltage [1]. Notwithstanding the fact that most power transformers are highly reliable, failures occur during their operation,

which is undesirable and unacceptable for a power system. Such failures can also entail significant financial costs, exacerbation of safety issues, and unexpected interruptions in power supply to consumers. Therefore, early fault diagnostics and detection in power transformers, largely determining the reliability of the entire power system, while costing more than all other power grid equipment, require closer attention [2–5]. Generally, diagnostics costs are much less than repair costs, especially in the case of accidents.

Thus, identifying near-misses is an important and urgent problem. The diagnostics of power transformers and their operating modes not only reduce repair costs, but also prevent many process incidents [6–8]. Therefore, the major diagnostic aim is defining the possibility of further safe operation of the equipment.

Most power transformers are designed as oil-filled to improve their efficiency. The oil, therefore, acts as an arc-quenching, cooling, and insulating medium. Obviously, the reliability and durability of such a transformer directly depend on the oil condition, the electrophysical parameters of which deteriorate during operation because of moisture and thermal oxidative aging, since electrical, magnetic, and thermal loads continuously impact the oil in the transformer operation [9–12]. Thus, the most common dielectric in the energy sector–oil—is believed to conditionally report about 70% of information on the state of oil-filled equipment, including power transformers [13].

Therefore, reducing the likelihood of transformer failure with further emergency power outages requires continuous online oil diagnostics, i.e., developing measures for the timely monitoring of the oil properties directly in operating modes [14,15].

Currently, the most informative and frequently used techniques for early diagnostics of developing failures are as follows: 1: recording partial discharges (PD) in oil–paper insulation; and 2: physicochemical analysis of insulating liquids and gases. Obviously, both discharges in the gas inclusions of transformer oil and PDs in it cause oil decomposition, with the release of corresponding gaseous decomposition products. The degree of electrical equipment wear during its operation can actually be understood by the PD intensity, and various developing faults can be estimated by the gas concentration and its increase rate [16–19]. A detailed review of various applied offline and online transformer oil monitoring techniques is given in [16]. Many publications on the topic have been analyzed; the advantages and disadvantages of various techniques have been shown. Pandey et al. [17] provide an overview of basic techniques used for the online monitoring of oil quality in the operating transformer by the amount of gas dissolved inside. Conventional and new techniques for detecting faults were comparatively analyzed, which allows for the selection of the most effective way to diagnose dissolved gas in specific fault cases. Karandaeva et al. [18] consider the causes of PDs and their impact on the insulation conditions, and propose a real-time monitoring system using a generalized insulation condition and fault localization criterion containing an additional parameter of partial discharge intensity (PDI), characterizing the PD power and intensity. The proposed technique uses statistical toolkits available for PC. Thus, the analysis of these studies shows that known methods for the conventional transformer oil quality diagnostics have certain drawbacks, which requires developing new promising approaches to this problem-solving. Laskar et al. [19] propose to monitor humidity using a fiber optic sensor, and Khramshin et al. [20,21] study the specifics of transformer operating modes to be considered when justifying the diagnostic functions of the transformer technical condition continuous monitoring system, and describe the Minitrans diagnostic complex, which allows for the monitoring of the gas and moisture content in transformer oil.

Along with conventional techniques, there are other modern ways to monitor transformer oils: physicochemical diagnostics, liquid and gas chromatography, heat monitoring (infrared thermography), optical techniques (ultraviolet–visible, infrared, and NMR spectroscopy), thermal analysis, etc. [22–27]. Taib et al. [22] show the possibility of identifying power transformer faults by the extended use of polarization and depolarization current measurements, conducted on an oil sample of the operating power transformer. For each specific condition, the authors propose introducing a corresponding unique dimensionless

value of a depolarization factor that allows defining the fault type. Kang et al. [23] describe a new way to diagnose the aging of mineral insulating oils by measuring their complex optical and dielectric properties using terahertz spectroscopy.

Kalathiripi et al. [24] review the latest developments in the field of diagnosing the transformer oil quality by colorimetry, which allows for the monitoring of the oil contamination, degradation, or oxidation. Transformer oil monitoring systems based on the optical techniques such as UV–visible spectroscopy, Fourier-transform IR spectroscopy, and nuclear magnetic resonance (NMR) spectroscopy are described. Degeratu et al. [25] study various thermal and spectroscopic oil quality control systems, and Khramshin et al. [26] consider smart systems for the multiparameter diagnostics of the HV transformer equipment technical state by the oil condition. Kinkeldey et al. [27] propose a procedure for estimating the oil transformer aging by oil parameters using a new fuzzy logic algorithm. It is shown that, if required, the oil can be restored or replaced, while paper insulation, the key factor for determining the transformer aging, is irreplaceable. Thus, to estimate quality, a paper sample should be taken from the transformer. Therefore, the proposed algorithm uses fuzzy sets of oil parameters (acidity, interfacial tension, carbon dioxide and monoxide, breakdown voltage) to define the paper insulation polymerization degree.

An analysis of the considered ways to monitor aging transformer oils shows that each of them has certain shortcomings, the majority of which are the following: need for additional complex equipment, analysis duration, need for special chemical compounds, possibility of laboratory monitoring only, etc.

Thus, despite quite a large number of different monitoring systems, improving existing techniques for diagnosing the transformer oil properties, and developing new ones, are of a particular relevance. Obviously, the reliability of diagnosing the high-voltage oil-filled electrical equipment conditions depends on the appropriate technique selected. Therefore,, diagnostic techniques for the monitoring of current equipment state onsite under operating voltage and, preferably, normal operation, come to the fore.

2. Developing a New Technique for Oil Properties' Diagnostics

It is known that the transformer oil quality is largely determined by moisture content, so this information is the most relevant for the transformer condition diagnostics. To solve this problem, a new diagnostic technique is proposed, forming the basis for the transformer condition monitoring system. It is based on forming an additional high-frequency measuring loop using a constructive parasitic capacitance between the first inner row of LV winding and the core surface as a measuring capacitor cell, along with the existing low-frequency operating power loop. In this case, high-frequency low-voltage is used as a data signal carrier. A review of the scientific, technical, and patent literature shows that it is the first time such an approach is used to solve the problem set.

As a diagnosed object, consider a typical oil-filled transformer consisting of the following key components (Figure 1): 1—power transformer tank; 2—transformer oil; 3—core; 4—high-voltage (HV) winding; 5—low-voltage (LV) winding; 6—HV winding end (A); 7—LV winding end (a).

An analysis of the oil-filled transformer design facilitated the development of a new approach to the monitoring of the transformer gas–liquid component state, which indirectly characterizes the physical degradation of this component.

The proposed technical solution implies the formation of an additional high-frequency measuring loop that uses a stray parasitic capacitance as a measuring capacitor cell (MCC), along with the existing low-frequency working power loop. In this case, high-frequency low–voltage serves as a data signal carrier.

To eliminate the cross-impact of low-frequency high-voltage and high-frequency low-voltage circuits, the pilot high-frequency low–voltage is excited by a special coupling capacitor, with an output to the power feeder through an appropriate low-frequency choke [17,20].
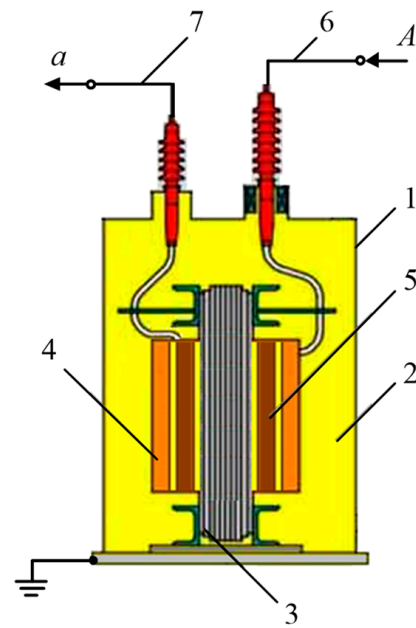
Figure 1. Structure flowchart of a high-voltage oil-filled power transformer.

Figure 2 shows the flowchart of the proposed system for monitoring the transformer components' parameters.
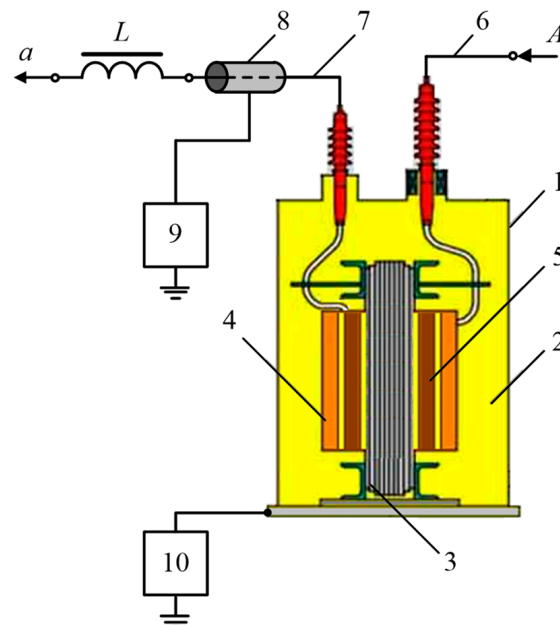

Figure 2. General flowchart of the transformer components' parameters monitoring system.

This flowchart comprises the following functional elements: 1—power transformer tank; 2—transformer oil; 3—core; 4—high-voltage (HV) winding; 5—low-voltage (LV) winding; 6—HV winding end; 7—LV winding end; 8—insulated cylindrical metal electrode with an inner coaxial LV winding end; 9—high-frequency sinusoidal low-voltage generator; 10—metering device; L—low-pass filter inductance; A—HV phase; a—LV phase.

Thus, the proposed technical control solution has the following benefits: (1) the oil can be diagnosed directly in real-time during operation under load; (2) several typical insulating oil parameters can be defined; (3) an LV HF sinusoidal voltage can be easily included in the HV LF power circuit; and (4) the transformer components can be used as the measuring system elements.

The last two features significantly simplify the entire measuring system for monitoring oil parameters inside the transformer tank.

The proposed technique also has certain drawbacks: 1: each control object requires the system operating modes to be individually adjusted while functional measuring modules are appropriately calibrated; and 2: the proposed monitoring system is focused on the design features of oil-filled transformers with the LV winding placed inside the HV one, which, in a certain sense, limits the applications of the monitoring system considered.

3. Analyzing Basic Physical Processes

To analyze the basic physical processes occurring in the transformer components in more detail, an equivalent circuit of an additional high-frequency measuring loop was built (Figure 3).
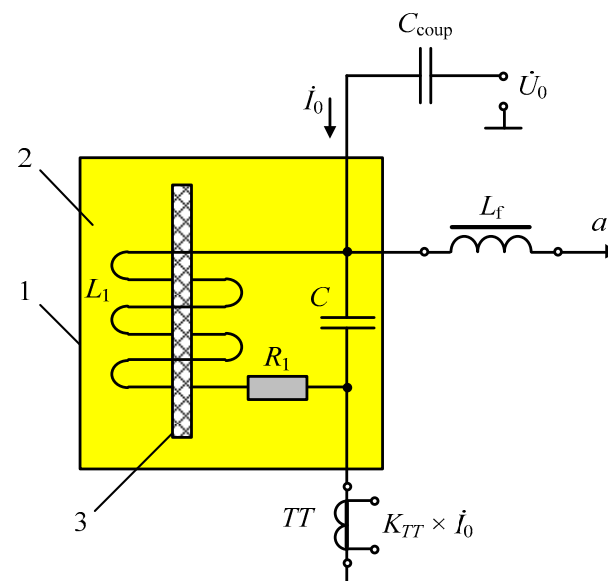
Figure 3. Equivalent circuit of the high-frequency measuring loop.

The equivalent circuit of an additional high-frequency measuring loop, shown in Figure 3, comprises the following components: C_{coup}—coupling capacitor formed by a cylindrical metal electrode and an inner coaxial winding end; L_f—the low-pass filter inductance (LF choke); $\dot{U}_0$—LV winding HF excitation voltages; $\dot{I}_0$—LV winding HF current; TT—measuring current transformer; K_{TT}—TT conversion rate; 1—a conditional elementary oil-filled transformer cell containing a core 2 and the LV winding active resistance R_1 and inductance L_1, as well as an MCC formed by a stray capacitance C between the LV winding's first inner row and the core surface.

To analyze physical processes in the circuit considered, assume that the LV winding and its core are cylindrical (Figure 4), and the LV winding's complex resistance

$$\dot{Z}_L = (R_1 + j \cdot \omega \cdot L_1) >> \dot{Z}_C, \tag{1}$$

where $\dot{Z}_C = -j \cdot \frac{1}{\omega \cdot C}$ is the MCC complex resistance; and ω is the LV winding's excitation voltage high cyclic frequency.

The assumptions made allow for the conclusion that $\dot{Z}_L \to \infty$, i.e., the LV winding's HF current $\dot{I}_0$ is actually determined by the parameters of the MCC with an impedance $\dot{Z}_C$.

Figure 4 shows the MCC design: 1—the MCC conditional tank; 2—the gas–liquid component; 3—metal core; 4—the LV winding's first inner row; 5—LV windings.
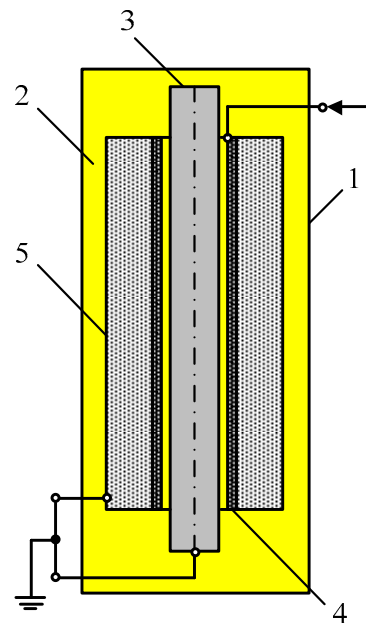
Figure 4. The MCC design.

In this case, the object monitored is a heterogeneous dissipative system with a variable physicochemical structure, filling the MCC conditional tank [23,26]. Such a type of dielcometric measuring capacitor cell is intended to monitor the composition and properties of filling substances. Its operating principle is based on the dependence between the physico–technological parameters of these substances and the measuring cell capacity.

With the aforementioned in mind, consider a simplified MCC model as a single measuring two-electrode cylindrical capacitor with an unfilled interelectrode space (an air dielectric), whose electrodes are two coaxial cylinders with an axial length l (m), and conditional radii of the inner and outer electrodes r_i and r_{i+1} (m), respectively.

$$C = \varepsilon_0 \times \varepsilon_1 \times \frac{2\beta \times l}{\ln\left(\frac{r_{i+1}}{r_i}\right)}. \tag{2}$$

When an interelectrode space is filled with a heterogeneous dissipative system (a mix of air, transformer oil, and process water), the MCC model can, thus, be represented as three series-connected two-electrode cylindrical capacitors C_1, C_2, and C_3, with different dielectrics: 1—air; 2—transformer oil; 3—process water, respectively (Figure 5).
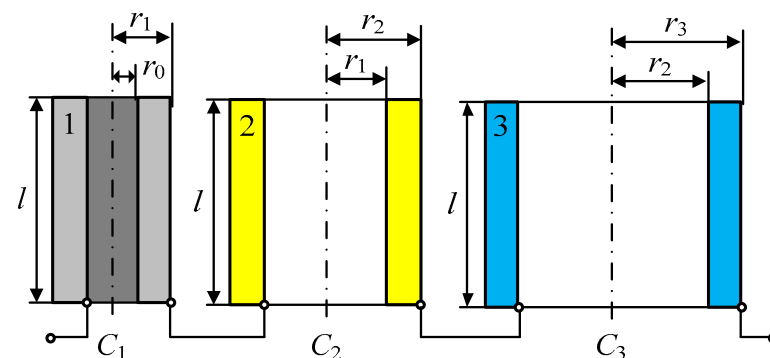

Figure 5. The electrical MCC model.

In this case, the electrical capacitance of each aforementioned capacitor can be consequently expressed by the following equations:

$$C_1 = \varepsilon_0 \times \varepsilon_1 \times \frac{2\pi \times l}{\ln\left(\frac{r_1}{r_0}\right)}; \quad C_2 = \varepsilon_0 \times \varepsilon_2 \times \frac{2\pi \times l}{\ln\left(\frac{r_2}{r_1}\right)}; \quad C_3 = \varepsilon_0 \times \varepsilon_3 \times \frac{2\pi \times l}{\ln\left(\frac{r_3}{r_2}\right)}, \tag{3}$$

where r_0 and r_1 are the radii of the C_1 air-filled capacitor's inner and outer electrodes, respectively; r_2 is the radius of the C_2 transformer oil-filled capacitor's outer electrode; r_3 is the radius of the C_3 process water-filled capacitor's outer electrode; ε_1 is the air permittivity; ε_2 is the transformer oil permittivity; and ε_3 is the process water permittivity.

Determining the reciprocal of the MCC's total capacitance:

$$
\begin{aligned}
\frac{1}{C} &= \frac{1}{2\pi \times \varepsilon_0 \times l} \times \left[\ln\left(\frac{r_1}{r_0}\right) + \frac{\ln\left(\frac{r_2}{r_1}\right)}{\varepsilon_2} + \frac{\ln\left(\frac{r_3}{r_2}\right)}{\varepsilon_3}\right] = \\
&= \frac{1}{2\pi \times \varepsilon_0 \times l} \times \left[\ln r_1 - \ln r_0 + \frac{\ln r_2 - \ln r_1}{\varepsilon_2} + \frac{\ln r_3 - \ln r_2}{\varepsilon_3}\right].
\end{aligned}
\tag{4}
$$

Assume that $d_1 = (r_1 - r_0)$ is the thickness of the air layer in the transformer oil that is conditionally uniformly spread over the electrode surface; $d_2 = (r_2 - r_1)$ is the thickness of the transformer oil layer, conditionally uniformly spread over the electrode surface; $d_3 = (r_3 - r_2)$ is the thickness of the water layer in the transformer oil, conditionally uniformly spread over the electrode surface; and $D = (d_1 + d_2 + d_3)$ is the average gap between the LV winding first inner row and the core surface.

Further, considering that $0 < r_{i+1}/r_i \leq 2$, Equation (4) can be reduced to:

$$\frac{1}{C} = \frac{1}{2\pi \times \varepsilon_0 \times l} \times \left[D - \frac{\varepsilon_2 - 1}{\varepsilon_2} \times d_2 - \frac{\varepsilon_3 - 1}{\varepsilon_3} \times d_3\right]. \tag{5}$$

Determining the MCC total capacitance according to (5)

$$C = \frac{2\pi \times \varepsilon_0 \times l}{D - \frac{\varepsilon_2 - 1}{\varepsilon_2} \times d_2 - \frac{\varepsilon_3 - 1}{\varepsilon_3} \times d_3}. \tag{6}$$

It is known that the volume resistance for a dielectric material in the interelectrode space of a cylindrical capacitor with coaxial electrodes is determined by the equation:

$$G_{DM} = g_v \times \frac{\ln\frac{r_{i+1}}{r_i}}{2\pi l} = g_v \times \frac{d}{2\pi l}, \tag{7}$$

where d is the layer thickness of the material in the cylindrical capacitor's interelectrode space; l is the axial length of the cylindrical capacitor electrodes; and g_v is the material specific volume resistance.

Considering Equation (7), Equation (6) can be rewritten in the form:

$$C = \frac{2\pi \times \varepsilon_0 \times l}{D - \frac{\varepsilon_2 - 1}{\varepsilon_2} \times \frac{2\pi \times l \times G_2}{g_2} - \frac{\varepsilon_3 - 1}{\varepsilon_3} \times \frac{2\pi \times l \times G_3}{g_3}}. \tag{8}$$

Determining the MCC impedance:

$$
\begin{aligned}
\dot{Z}_{C_1} &= -j \times \frac{1}{\omega \times C} = -j \times \frac{1}{2\pi \times \omega \times \varepsilon_0 \times l} \times \rightarrow \\
&\rightarrow \times \left(D - \frac{\varepsilon_2 - 1}{\varepsilon_2} \times \frac{2\pi \times l \times G_2}{g_2} - \frac{\varepsilon_3 - 1}{\varepsilon_3} \times \frac{2\pi \times l \times G_3}{g_3}\right)
\end{aligned}
\tag{9}
$$

Representing the permittivity as a complex, according to the Debye theory:

$$\dot{\varepsilon} = \varepsilon' - j \times \varepsilon'', \tag{10}$$

where ε' is the real component of the complex permittivity characterizing the system polarity; and ε'' is the imaginary component of the complex permittivity characterizing the

electric field energy absorption by the system via various channels, including reach-through conductivity.

Considering (10), we can write Equation (9) as follows:

$$
\begin{aligned}
\dot{Z}_C &= -j \times \tfrac{1}{2\pi \times \omega \times \varepsilon_0 \times l} \times \rightarrow \\
&\rightarrow \times \left(D - \tfrac{(\varepsilon_2' - j \times \varepsilon_2'' - 1)}{(\varepsilon_2' - j \times \varepsilon_2'')} \times \tfrac{2\pi \times l \times G_2}{g_2} - \tfrac{(\varepsilon_3' - j \times \varepsilon_3'' - 1)}{(\varepsilon_3' - j \times \varepsilon_3'')} \times \tfrac{2\pi \times l \times G_3}{g_3} \right) = \\
&= -j \times \tfrac{1}{2\pi \times \omega \times \varepsilon_0 \times l} \times \rightarrow \\
&\rightarrow \times \left\{ D - \tfrac{2\pi \times l \times G_2}{g_2} \times \left(1 - \tfrac{\varepsilon_2'}{(\varepsilon_2')^2 + (\varepsilon_2'')^2} - j \times \tfrac{\varepsilon_2''}{(\varepsilon_2')^2 + (\varepsilon_2'')^2} \right) - \rightarrow \right. \\
&\left. \rightarrow -\tfrac{2\pi \times l \times G_3}{g_3} \times \left(1 - \tfrac{\varepsilon_3'}{(\varepsilon_3')^2 + (\varepsilon_3'')^2} - j \times \tfrac{\varepsilon_3''}{(\varepsilon_3')^2 + (\varepsilon_3'')^2} \right) \right\} = \\
&= -j \times \tfrac{1}{2\pi \times \omega \times \varepsilon_0 \times l} \times \rightarrow \\
&\rightarrow \times \left\{ D - \tfrac{2\pi \times l \times G_2}{g_2} \times \left(1 - \tfrac{\varepsilon_2'}{(\varepsilon_2')^2 + (\varepsilon_2'')^2} \right) - \rightarrow \right. \\
&\rightarrow -\tfrac{2\pi \times l \times G_3}{g_3} \times \left(1 - \tfrac{\varepsilon_3'}{(\varepsilon_3')^2 + (\varepsilon_3'')^2} \right) + \rightarrow \\
&\rightarrow +j \times \left[\begin{array}{l} \tfrac{2\pi \times l \times G_2}{g_2} \times \left(\tfrac{\varepsilon_2''}{(\varepsilon_2')^2 + (\varepsilon_2'')^2} \right) + \rightarrow \\ \rightarrow +\tfrac{2\pi \times l \times G_3}{g_3} \times \left(\tfrac{\varepsilon_3''}{(\varepsilon_3')^2 + (\varepsilon_3'')^2} \right) \end{array} \right] \left. \right\} = \\
&= \tfrac{1}{2\pi \times \omega \times \varepsilon_0 \times l} \times \left\{ \begin{array}{l} \tfrac{2\pi \times l \times G_2}{g_2} \times \left(\tfrac{\varepsilon_2''}{(\varepsilon_2')^2 + (\varepsilon_2'')^2} \right) + \rightarrow \\ \rightarrow +\tfrac{2\pi \times l \times G_3}{g_3} \times \left(\tfrac{\varepsilon_3''}{(\varepsilon_3')^2 + (\varepsilon_3'')^2} \right) \end{array} - \rightarrow \right. \\
&\left. \rightarrow -j \times \left[\begin{array}{l} D - \tfrac{2\pi \times l \times G_2}{g_2} \times \left(1 - \tfrac{\varepsilon_2'}{(\varepsilon_2')^2 + (\varepsilon_2'')^2} \right) - \rightarrow \\ \rightarrow -\tfrac{2\pi \times l \times G_3}{g_3} \times \left(1 - \tfrac{\varepsilon_3'}{(\varepsilon_3')^2 + (\varepsilon_3'')^2} \right) \end{array} \right] \right\}
\end{aligned}
\tag{11}
$$

After a series of simple transformations, Equation (11) is easily transformed into:

$$
\dot{Z}_C = (b_2 \times G_2 + b_3 \times G_3) - j \times (a_0 - a_2 \times G_2 - a_3 \times G_3) = B - j \times A, \tag{12}
$$

where $a_0 = \frac{D}{2\pi \times \omega \times \varepsilon_0 \times l}$, $a_2 = \frac{1}{\omega \times \varepsilon_0 \times g_2} \times \left(1 - \frac{\varepsilon_2'}{(\varepsilon_2')^2 + (\varepsilon_2'')^2} \right)$, $a_3 = \frac{1}{\omega \times \varepsilon_0 \times g_3} \times \left(1 - \frac{\varepsilon_3'}{(\varepsilon_3')^2 + (\varepsilon_3'')^2} \right)$, $b_2 = \frac{1}{\omega \times \varepsilon_0 \times g_2} \times \left(\frac{\varepsilon_2''}{(\varepsilon_2')^2 + (\varepsilon_2'')^2} \right)$ and $b_3 = \frac{1}{\omega \times \varepsilon_0 \times g_3} \times \left(\frac{\varepsilon_3''}{(\varepsilon_3')^2 + (\varepsilon_3'')^2} \right)$—constant coefficients; $B = (b_2 \times G_2 + b_3 \times G_3)$ and $A = (a_0 - a_2 \times G_2 - a_3 \times G_3)$ are the active and reactive components of the MCC impedance, respectively.

According to (12), building a system of linearly independent algebraic equations:

$$
\begin{cases} B = b_2 \times G_2 + b_3 \times G_3; \\ A = a_0 - a_2 \times G_2 - a_3 \times G_3. \end{cases} \tag{13}
$$

The solution to the system of Equation (13) is mathematically expressed as follows:

$$
G_2 = \frac{A \times b_3 - a_0 \times b_3 + a_3 \times B}{a_3 \times b_2 - a_2 \times b_3} \text{ and } G_3 = \frac{a_0 \times b_2 \times b_3 - a_2 \times b_3 \times (B + A)}{b_3 \times (a_3 \times b_2 - a_2 \times b_3)}. \tag{14}
$$

To determine the MCC conductivity:

$$
\frac{1}{\dot{Z}_C} = \frac{1}{B - j \times A} = \frac{B}{A^2 + B^2} + j \times \frac{A}{A^2 + B^2} = \dot{Q}_a + \dot{Q}_p, \tag{15}
$$

where $\dot{Q}_a = \frac{B}{A^2+B^2}$ and $\dot{Q}_p = j \times \frac{A}{A^2+B^2}$ are the MCC active and reactive conductivities, respectively.

According to (15), the (passive two-pole) measuring capacitor cell C can be represented as an equivalent circuit consisting of parallel active $\dot{Q}_a$ and reactive $\dot{Q}_p$ conductivity components, and the total electric current $\dot{I}_0$ in it can be expressed through its two active $\dot{I}_a$ and reactive $\dot{I}_p$ components (Figure 6):

$$\dot{I}_0 = \dot{U}_C \times \frac{1}{\dot{Z}_C} = \dot{U}_C \times \dot{Q}_a + \dot{U}_C \times \dot{Q}_p = \dot{I}_a + \dot{I}_p, \tag{16}$$

where $\dot{I}_a = \dot{U}_C \times \dot{Q}_a$ and $\dot{I}_p = U_C \times \dot{Q}_p$ are, respectively, the active and reactive components of the circuit total HF electric current $\dot{I}_0$; and $\dot{U}_C = U_C \times e^{j\phi_{uc}} = \dot{U}_0 - \dot{I}_0 \times \dot{Z}_c$ is the HF voltage applied to the MCC.
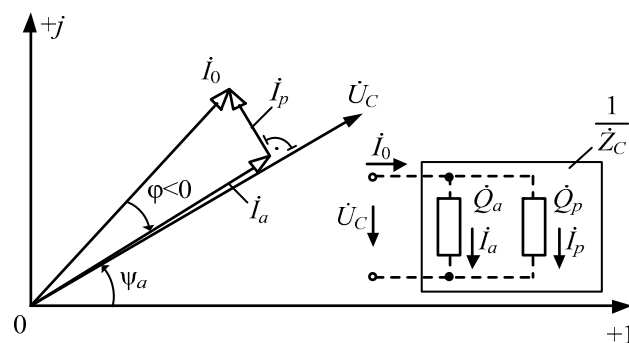

Figure 6. Vectogram of HF voltages and currents.

To simultaneously form scalar components from a vector quantity $\dot{I}_0$, proportional to its projections on the corresponding coordinate axes, or its phase relative to another vector quantity $\dot{U}_C$, the simplest quadrature functional converters are used—quadrature synchronous detectors (*SD*), with reference voltages shifted by $\pi/2$ in phase.

When aligning the *SDs'* reference voltage vectors with the coordinate axes on the complex plane $\dot{U}_C$, the constant components of the circuit rectified electric current at the outputs of *SDs* operating in key modes are defined as follows:

$$\begin{cases} I_a = K \times \left|\dot{I}_0\right| \times \cos(\arg \dot{I}_0); \\ I_p = K \times \left|\dot{I}_0\right| \times \sin(\arg \dot{I}_0), \end{cases} \tag{17}$$

where I_a and I_p are the recorded effective values of the active and reactive components of the circuit's total HF current $\dot{I}_0$, respectively; $K = K_{TT} \times K_{SD}$; K_{TT}, and K_{SD} are the *TT* and quadrature *SD* conversion rates, respectively; and $(\arg \dot{I}_0)$ is the angle between the *SD*'s input and reference voltages.

Based on (16) and (17), the effective values of active and reactive conductivities are defined, respectively, as:

$$Q_a = \frac{I_a}{K \times U_C} = \frac{B}{A^2 + B^2} \text{ and } Q_p = \frac{I_p}{K \times U_C} = \frac{A}{A^2 + B^2}. \tag{18}$$

Considering $B/Q_a = A/Q_p$, the effective values of the MCC impedance active and reactive components can be written, respectively, as:

$$A = \frac{Q_p}{(Q_p^2 + Q_a^2)} \text{ and } B = \frac{Q_a}{(Q_p^2 + Q_a^2)} \tag{19}$$

After simple transformations of Equation (19), we eventually obtain:

$$A = \frac{I_p}{K \times U_C} \times \frac{K^2 \times U_C^2}{(I_p^2 + I_a^2)} = \frac{K \times U_C \times I_p}{(I_p^2 + I_a^2)} \text{ and } B = \frac{I_a}{K \times U_C} \times \frac{K^2 \times U_C^2}{(I_p^2 + I_a^2)} = \frac{K \times U_C \times I_a}{(I_p^2 + I_a^2)} \tag{20}$$

Appropriately substituting (20) into (14), the volume resistance for transformer oil and technical water in the MCC interelectrode space is defined as:

$$G_2 = \frac{K \times U_C \times I_p \times b_3 + K \times U_C \times I_a \times a_3 - a_0 \times b_3 \times (I_p^2 + I_a^2)}{(I_p^2 + I_a^2) \times (a_3 \times b_2 - a_2 \times b_3)} \tag{21}$$

$$G_3 = \frac{a_0 \times b_2 \times b_3 \times (I_p^2 + I_a^2) - a_2 \times b_3 \times K \times U_C \times (I_a + I_p)}{(I_p^2 + I_a^2) \times b_3 \times (a_3 \times b_2 - a_2 \times b_3)} \tag{22}$$

Taking into account the MCC resonant excitation mode in the circuit considered, we can assume that $U_C = U_0$.

The analysis of algorithms for obtaining the current resistances (21) and (22) of transformer oil (TO) and process water (PW) allows the conclusion that the composition of the complex heterogeneous liquid mix in the power transformer tank can actually be monitored by forming an additional HF measuring loop (AHFML) in its operating electrical circuit.

If, due to the impact of various operational and time factors, the algorithmically determined values of the heterogeneous liquid mix component parameters exceed the corresponding reference limits, this indicates certain degradation processes occurring in the functional elements of that power equipment. Continuous monitoring of the specified oil parameters allows for the early diagnostics of destructive processes and thereby, a timely arrangement of appropriate measures to eliminate them, or replace the oil in the transformer tank [17,26].

4. Structure Flowchart of an Additional HF Measuring Loop

Figure 7 shows a variant of the AHFML's structure flowchart, where $\dot{U}_0$ is the AHFML HF power voltage; U_0 is the effective value of the AHFML power voltage; $\dot{Z}_{coup}$ is the coupling capacitor's complex resistance; $\dot{Z}_C$ is the MCC complex resistance; $\dot{I}_0$ is the AHFML HF current; I_a and I_p are the measured effective values of the $\dot{I}_0$ active and reactive components, respectively; K_{TT} is the measuring *TT's* conversion rate; $K = K_{TT} \times K_{SD}$ is the measuring channel conversion rate, K_{SD} is the synchronous detector conversion rate; a_i are preset design parameters; 1 is the measuring current transformer; 2 is the current meter; 3 and 4 are quadrature synchronous detectors; 5 is the reference voltage generator for synchronous detectors; and 6 is the data processing unit.
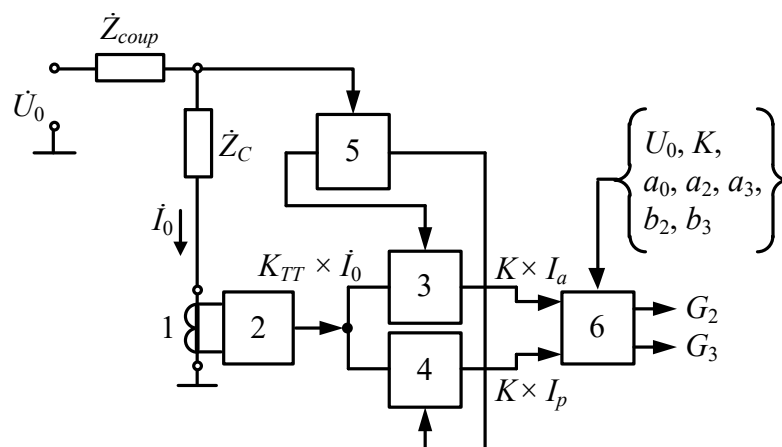

Figure 7. The AHFML's structure flowchart.

In fact, the AHFML is formed by a set of functional elements, $1 \div 6$, conducting the secondary processing of the data signal generated by an MCC with the impedance $\dot{Z}_C$. The AHFML is powered with HF voltage $\dot{U}_0$ from the corresponding power source through the coupling capacitor C_{coup}, with the impedance $\dot{Z}_{coup}$.

5. Experimental Verification

The operability and efficiency of the proposed monitoring system were verified by the appropriate experimental studies, where a power transformer TM-25-6/0.4 filled with a liquid transformer oil TKp (TU 38.101890–81) was used as a monitored object, and moisture content in the transformer oil H was selected as the studied parameter. Experimental studies were performed at a constant ambient temperature (25 °C) and a transformer load current of 25 A in the transformer's steady-state operating mode.

Note that for the moisture content in oil H, a phenomenological dependence corresponding to the Equation (7) was used:

$$H = \frac{M_3}{M_2} \propto \frac{G_3}{G_2}, \tag{23}$$

where M_3 and M_2 are the masses of process water and transformer oil, respectively.

Eight specially prepared oil–water liquid mix samples were used in the experimental studies, i.e., a kind of water-in-oil emulsion (w/o reverse type), where the dispersion medium and phase were, respectively, oil and water. For each sample, the weight fractions of the dispersion medium and phase were predetermined separately by gravity, i.e., weighing on electronic scales, with further preparation of the sample itself using a special emulsifier. In this case, it was assured that the required moisture content H_i was set, and subsequently defined using the proposed indirect HF impedance technique. After that, the prepared samples were placed in the transformer tank in a certain sequence.

The required data signals were registered by the AHFML, and algorithmically processed to determine the current moisture content as the corresponding measurement result. In other words, based on 10moisture content observation data for each sample $\{H_{ij}\}$ ($i = 1 \div 8$—the sample number, $j = 1 \div 10$—the observation data number for the i-th sample), the corresponding measurement result was defined as the arithmetic mean of an observation data group $\{H_i^*\}$ for each sample prepared.

Table 1 contains the generalized results of experimental studies to identify whether it is feasible to obtain the moisture content H in transformer oil using the AHFML.

Table 1. Experimental study results.

Sample No. i	Preset Value H_i (ppm)	Measurement Result H_i^* (ppm)	δ (%)
1	5	6.25	25
2	10	11.4	14
3	15	16.65	11
4	20	21.8	9
5	25	27	8
6	30	32.25	7.5
7	35	37.21	6.3
8	40	42.4	6

When analyzing the observation data, the corresponding ratios of the statistical characteristics of the output AHFML were used.

Based on the experimental data analysis, the authors built a curve illustrating the relative error δ of defining the current moisture content in oil (Figure 8), where the X (0–H) and Y (0–δ) axes represent, respectively, the reference moisture content values of each liquid sample and the error of the corresponding reference moisture content values measured using the technique proposed.
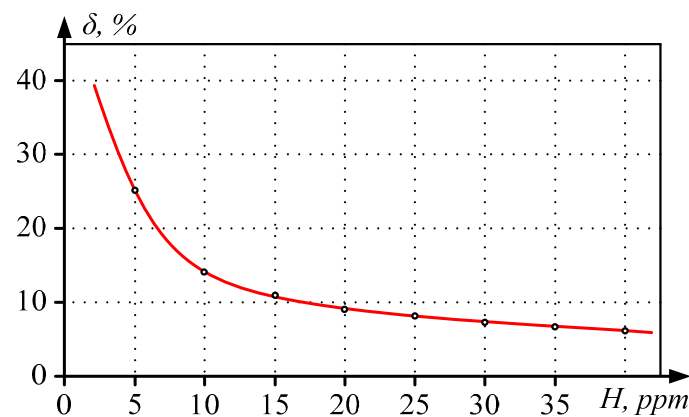
Figure 8. The relative error at *H* defining.

Note that the number of reference liquid mix sets (samples) was chosen according to the existing four classes of the oil technical condition. Given the complex sample preparation technology, this number is sufficient for correct experimental studies. Since the measurement result significance was estimated by the Fisher criterion, the moisture content was measured ten-fold for each reference sample, which ultimately ensured the required reliability of the entire experiment.

The oil condition was classified according to the moisture content, the presence of faults, and their development degree depending on the moisture content in the oil as follows:

1　　Normal, less than 5 ppm, i.e., no obvious faults;
2　　Working–Normal, with deviations less than 10 ppm, i.e., minor fault;
3　　Working–Normal, with significant deviations from 10 to 15 ppm, i.e., significant fault;
4　　Deteriorated condition, with deviations from 15 to 25 ppm, i.e., critical fault.

Figure 8 allows for the conclusion that critical faults can be identified by the increased moisture content in the oil with a maximum error of 10%, considering the aforementioned classification of the oil condition, and the AHFML sensitivity threshold reaches about tenths of ppm. Therefore, at a reduced moisture content *H* < 5%, the MCC operates in a mode close to its sensitivity threshold, which determines the trend towards decreasing the measurement accuracy in Figure 8.

The *δ*-*H* dependence nature indicates an additive measurement error associated with pickups, drifts, and vibrations. Further improvement of the AHFML design and technology will allow the full realization of the existing potential and the effective functioning of the entire system.

Although the paper sets the problem of defining the oil technical condition by the moisture content, to sum up, the proposed monitoring system allows for the defining of the following insulating oil parameters by means of the appropriate algorithm for processing the recorded data: 1—moisture content; 2—dielectric losses due to the accumulation of aging products in the oil and its pollution; and 3—the content of gases dissolved in oil.

According to Figure 6 and Formula (17), the dielectric loss tangent is determined by the I_p/I_a ratio, and dielectric losses are defined by the equation:

$$P = U_C^2 \times \omega_p \times C \times \frac{I_p}{I_a} \tag{24}$$

where the total MCC capacitance *C* is defined by Equation (8).

6. Conclusions

The proposed system for monitoring the power transformer conditions, implementing an option of the HF impedance technique, not only allows the technical staff to make

timely and prompt decisions based on the data obtained, but also provides a long-term performance of the power equipment.

The proposed technique is effective, as it allows for building a power transformer failure prevention system. Such a system improves the reliability of state monitoring of the power oil-filled transformer, due to the early detection of incipient faults by the continuous monitoring of water and gases dissolved in oil. Another distinctive feature of the diagnostics proposed is the simplicity of its technical implementation, which does not compromise the integrity of the transformer structural elements and its operating mode.

However, it should be emphasized that the study does not involve the numerical estimating of the proposed technique accuracy against the already known methods. A detailed design of the circuit hardware part of the device, implementing the technique developed, its optimization, and thorough experimental studies, is the next independent stage of ongoing work. The research is aimed at identifying the essence of physical effects that allow for the monitoring of the oil condition directly during the transformer operation, by forming an additional HF measuring loop in its operating circuit and, theoretically, justifying the monitoring procedure. Thus, the study results in the new justified monitoring technique and its fundamental hardware implementation, currently unknown from the available technical information sources. This contributes to the development of the theory and practice of monitoring the power oil transformer conditions.

To conclude, it is of note that the proposed oil monitoring technique can be used to control not only transformers, but also other oil-filled power equipment, e.g., reactors, oil circuit breakers, current and voltage measuring transformers, HV bushings, etc.

Author Contributions: Conceptualization, I.V.B. (Igor V. Bochkarev) and I.V.B. (Ivan V. Bryakin); methodology, V.R.K.; software, V.R.G. and I.V.L.; validation, I.V.B. (Igor V. Bochkarev) and V.R.K.; formal analysis, V.R.G. All authors have read and agreed to the published version of the manuscript.

Institutional Review Board Statement: Not applicable.

Informed Consent Statement: Not applicable.

Data Availability Statement: Not applicable.

Conflicts of Interest: The authors declare no conflict of interest.

References

1. Werle, P.; Brendel, H. Transformers. In *Springer Handbook of Power Systems*; Springer Handbooks; Springer: Singapore, 2021; pp. 443–509. [CrossRef]
2. Šimková, M.; Ministr, M.; Hammer, M. Expert Systems in Transformer Diagnostics. In *Recent Advances in Mechatronics*; Springer: Berlin/Heidelberg, Germany, 2010; pp. 145–150. [CrossRef]
3. Singh, R.P.; Sonawane, A.V.; Satpute, M.S.; Shirsath, D.Y.; Thakre, M.A. Review on Traditional Methods of Condition Monitoring of Transformer. In Proceedings of the International Conference on Electronics and Sustainable Communication Systems (ICESC), Coimbatore, India, 2–4 July 2020; pp. 1144–1152. [CrossRef]
4. Kim, Y.; Park, T.; Kim, S.; Kwak, N.; Kweon, D. Artificial Intelligent Fault Diagnostic Method for Power Transformers using a New Classification System of Faults. *J. Electr. Eng. Technol.* **2019**, *14*, 825–831. [CrossRef]
5. Auronen, T.; Murat, I.; Hanninen, T.; Keitoue, S. Future Trends in Transformer Online Monitoring. *Lect. Notes Electr. Eng.* **2020**, *671*, 55–66. [CrossRef]
6. Patel, D.; Chothani, N. Real-Time Monitoring and Adaptive Protection of Power Transformer. In *Digital Protective Schemes for Power Transformer*; Springer Handbooks; Springer: Singapore, 2020; pp. 173–190. [CrossRef]
7. Zhi-Hua, Z.; Yuan, J.; Xu-Ri, Y.; Shi-Fu, C. The Application of Visualization and Neural Network Techniques in a Power Transformer Condition Monitoring System. *Lect. Notes Electr. Eng.* **2002**, *2358*, 325–334. [CrossRef]
8. Islam, M.; Lee, G.; Hettiwatte, S.N. A review of condition monitoring techniques and diagnostic tests for lifetime estimation of power transformers. *Electr. Eng.* **2018**, *100*, 581–605. [CrossRef]
9. Wilson, A.C.M. *Insulating Liquids: Their Uses, Manufacture and Properties*; Peter Peregrinus LTD: London, UK; New York, NY, USA, 1980; 221p.
10. Fofana, I.; Borsi, H.; Gochenbach, J. Fundamental investigation on some transformer liquids under various outdoor conditions. *IEEE Trans. Dielec. Electric. Insulat.* **2001**, *8*, 1040–1047. [CrossRef]

11. Kathik, R.; Raja, T.S.R. Investigations of transformer oil characteristics. *IEEJ Trans. Electr. Electron. Eng.* **2012**, *7*, 2543–2553. [CrossRef]

12. Abdi, S.; Safiddine, L.; Boubakeur, A.; Haddad, A. The Effect of Water Content on the Electrical Properties of Transformer Oil. *Lect. Notes Electr. Eng.* **2019**, *599*, 518–527. [CrossRef]

13. Sokolov, V.; Bassetto, A.; Oommen, T.V.; Haupert, T.; Hanson, D. Transformer fluid: A powerful tool for the life management of an ageing transformer population. In Proceedings of the TechCon Asia-Pacific Conference, Sidney, Australia, 7–9 May 2003; pp. 1–19.

14. Schreiter, S.; Lohmeyer, H.; Werle, P. Multidimensional Analysis of a Real Transformer Fleet Based on the Evaluation of Oil Properties. *Lect. Notes Electr. Eng.* **2019**, *598*, 697–704. [CrossRef]

15. Negi, J.; Maithani, G. Power Transformer Condition Assessment through Insulating Oil Testing. In *Proceedings of Integrated Intelligence Enable Networks and Computing*; Algorithms for Intelligent Systems; Springer: Singapore, 2021; pp. 161–170. [CrossRef]

16. Rengaraj, R.; Venkatakrishnan, G.R.; Moorthy, P.; Pratyusha, R. Transformer Oil Health Monitoring Techniques—An Overview. *Adv. Smart Syst. Technol.* **2021**, *1163*, 135–154. [CrossRef]

17. Pandey, R.; Soni, P.; Goel, N.; Shukla, S.P.; Saji, T.C. Condition Monitoring of Power Transformer by Dissolved Gas Analysis: A Review. *Adv. Power Syst. Energy Manag.* **2021**, *690*, 289–298. [CrossRef]

18. Karandaeva, O.I.; Yakimov, I.A.; Filimonova, A.A.; Gartlib, E.A.; Yachikov, I.M. Stating Diagnosis of Current State of Electric Furnace Transformer on the Basis of Analysis of Partial Discharges. *Machines* **2019**, *7*, 77. [CrossRef]

19. Laskar, S.; Bordoloi, S. Monitoring of moisture in transformer oil using optical fiber as sensor. *J. Photonics* **2013**, *2013*, 528478. [CrossRef]

20. Karandaev, A.S.; Evdokimov, S.A.; Khramshin, V.R.; Lednov, R.A. Diagnostic Functions of a System for Continuous Monitoring of the Technical Condition of the Transformers of Arc Steelmaking Furnaces. *Metallurgist* **2014**, *58*, 655–663. [CrossRef]

21. Karandaev, A.S.; Evdokimov, S.A.; Khramshin, V.R.; Sarlybaev, A.A. System for Real-Time Monitoring of the Technical State of a Transformer on an Ultrahigh-Power Electric-Arc Steelmaking Furnace. *Metallurgist* **2014**, *58*, 872–879. [CrossRef]

22. Taib, M.A.; Nor, A.M.; Zulkurnain, A.R.; Mohd, N.A. Depolarization Ratio Index (DRI) as alternative method in identifying oil-filled transformer internal faults. *Electr. Eng.* **2021**, *103*, 2685–2704. [CrossRef]

23. Kang, S.B.; Kim, W.S.; Chung, D.C.; Joung, J.M. Degradation diagnosis of transformer insulating oils with terahertz time-domain spectroscopy. *J. Korean Phys. Soc.* **2017**, *71*, 986–992. [CrossRef]

24. Kalathiripi, H.; Karmakar, S. Analysis of transformer oil degradation due to thermal stress using optical spectroscopic techniques. *Int. Trans. Electr. Energ. Syst.* **2017**, *27*, 2346. [CrossRef]

25. Degeratu, S.; Rotaru, P.; Rizescu, S.; Danoiu, S.; Bizdaoca, N.G.; Alboteanu, L.I.; Manolea, H.O. Condition monitoring of transformer oil using thermal analysis and other techniques. *J. Therm. Anal. Calorim.* **2015**, *119*, 1679–1692. [CrossRef]

26. Khramshin, V.R.; Evdokimov, S.A.; Nikolaev, A.A.; Karandaev, A.S. Monitoring Technical State of the Power Transformers Is a Necessary Condition of the Smart-Grid Technology Introduction within the Industrial Electric Networks. In Proceedings of the IEEE NW Russia Young Researchers in Electrical and Electronic Engineering Conference, St. Petersburg, Russia, 2–4 February 2015; pp. 214–220. [CrossRef]

27. Kinkeldey, T.; Münster, T.; Werle, P.; Hämel, S.K.; Preusel, J. Estimation of the Ageing Condition of Oil-Filled Transformers Based on the Oil Parameters Using a Novel Fuzzy Logic Algorithm. *Lect. Notes Electr. Eng.* **2020**, *598*, 926–936. [CrossRef]